AGU PUBLICATIONS

JGR

Journal of Geophysical Research: Space Physics

RESEARCH ARTICLE
10.1002/2014JA019835

Key Points:
- NEIALs show very strong aspect angle dependence
- The level of dependence is determined by NEIALs' generation mechanism
- Multiple mechanisms can be simultaneously generating NEIALs

Supporting Information:
- Readme
- Movie S1

Correspondence to:
H. Akbari,
hakbari@bu.edu

Citation:
Akbari, H., and J. L. Semeter (2014), Aspect angle dependence of naturally enhanced ion acoustic lines, *J. Geophys. Res. Space Physics*, *119*, 5909–5917, doi:10.1002/2014JA019835.

Received 28 JAN 2014
Accepted 2 JUL 2014
Accepted article online 5 JUL 2014
Published online 22 JUL 2014

Aspect angle dependence of naturally enhanced ion acoustic lines

H. Akbari[1] and J. L. Semeter[1]

[1]Department of Electrical and Computer Engineering and Center for Space Physics, Boston University, Boston, Massachusetts, USA

Abstract The magnetic aspect angle dependence of naturally enhanced ion acoustic lines (NEIALs) is investigated using two multibeam experiments with the 450 MHz electronically steerable Poker Flat Incoherent Scatter Radar. In each experiment, dynamics in the accompanying auroral activity suggest that the source of free energy for the instability is equally present, in a statistical sense, in a wide portion of sky. Yet strong variations in backscattered power are observed when radar beam direction is altered by only 1°. In our observations, the strongest scattered power appears in the magnetic-zenith direction and weakens with increasing angle between the radar beam and the magnetic lines of force. NEIALs occurring above the *F* region peak are observed to disappear almost completely at aspect angles as small as 2°. The results are somewhat surprising since previous experiments have detected NEIALs at aspect angles up to 15°. It is shown that during dynamic geophysical conditions, such as the substorm intervals studied in this report, more than one of the generation mechanisms proposed to explain NEIALs may be operating simultaneously. The different mechanisms result in different spectral morphologies and different degrees of sensitivity to the magnetic aspect angle.

1. Introduction

Ever since the first observation by *Foster et al*. [1988], the appearance of strong nonthermal echoes in incoherent scatter radar (ISR) data has been the subject of numerous theoretical and experimental studies. Localization of the increased received power at the expected frequency of the ion acoustic resonance confirms that such echoes are the result of scattering by destabilized ion acoustic waves. Hence, the name "naturally enhanced ion acoustic lines" (NEIALs) has been used to refer to these echoes. Different mechanisms have been proposed to explain NEIALs. These include (1) streaming instabilities due to relative drifts between thermal electrons and different species of ions [*Rietveld et al*., 1991; *Collis et al*., 1991; *Wahlund et al*., 1992], (2) wave-wave interactions where a destabilized primary Langmuir wave gives rise to enhanced ion acoustic waves [*Forme*, 1993, 1999; *Strømme et al*., 2005], and (3) destabilization of ion acoustic waves by local acceleration of electrons by ion cyclotron waves [*Bahcivan and Cosgrove*, 2008]. Regardless of the generation mechanism, the initial free energy is assumed to be provided by electron precipitation. Since auroral activity is a proxy for electron precipitation, some experimental works have been focused on correlating radar echoes with optical data and investigating the temporal and spatial relationship between NEIALs and different types of aurora [*Collis et al*., 1991; *Sedgemore-Schulthess et al*., 1999; *Grydeland et al*., 2003, 2004; *Blixt et al*., 2005; *Michell et al*., 2008, 2009; *Michell and Samara*, 2010]. Other efforts have focused on the statistical occurrence of NEIALs as a function of altitude, season, and radar frequency [*Rietveld et al*., 1991, 1996].

One aspect of NEIALs that has not been systematically investigated is their dependence on magnetic aspect angle. The degree to which the visibility of NEIALs changes with magnetic aspect angle depends on the underlying generation mechanism. For instance, streaming instabilities produced by field-aligned particle fluxes are expected to destabilize ion acoustic waves in a highly field-aligned fashion, whereas ion acoustic wave enhancements generated by parametric decay of Langmuir waves should be observable over a wide range of angles to the magnetic field lines (as discussed further in section 3). The aspect angle dependence of NEIALs therefore provides an additional constraint on possible generation mechanisms. The lack of experimental work on this matter is in part due to the ephemeral nature of the echoes coupled with limitations in beam-steering speed associated with dish-based ISRs. However, the pulse-by-pulse steering capability of the new Advanced Modular Incoherent Scatter Radars is well suited for such studies.

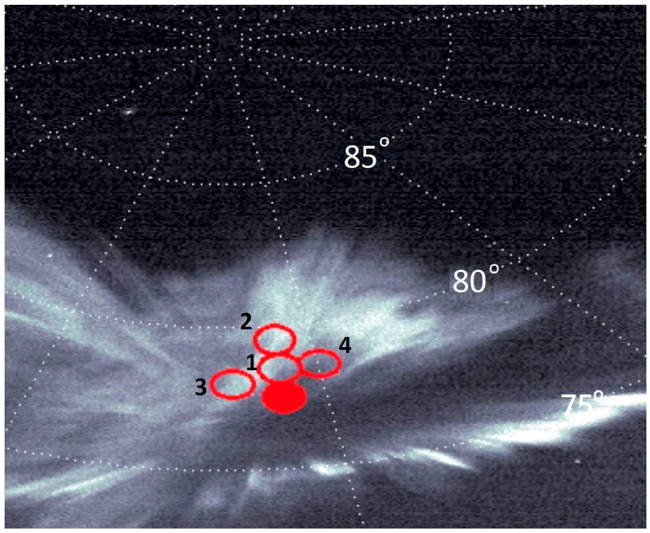

Figure 1. PFISR beam positions overlain on one frame recorded by a narrow-field camera on 1 March 2011. The magnetic-zenith beam is filled in; the separation between beams is 1° [after *Dahlgren et al*., 2013].

In this study, the multibeam capability of the 450 MHz Poker Flat Incoherent Scatter Radar (PFISR; 65.12°N, 147.47°W) is exploited to investigate the visibility and intensity of NEIALs as a function of magnetic aspect angle. NEIALs are known to be localized in space with small horizontal scales (about 100 m) [*Cabrit et al*., 1996; *Grydeland et al*., 2004]. Since different beam directions intersect different locations in space, it is possible to mistakenly interpret spatial variability in the NEIAL source as a magnetic aspect angle effect. To distinguish between these cases, we monitor auroral activity as a proxy for the spatial distribution of the underlying turbulence. The present work concerns NEIALs observed during substorm expansion phase, wherein dynamic auroral forms moved rapidly through the set of radar beams and later covered a large portion of sky. It is therefore argued that differences in echo characteristics in the different beams must be due to magnetic aspect angle.

2. Observations

An experiment was conducted during a 1 week period beginning 1 March 2011 with the specific aim of investigating the aspect angle dependence of NEIALs. PFISR was configured to sample five beam positions, one pointed to the magnetic zenith and four adjacent beams separated by only 1°. Figure 1 shows the position and angular extent (half-power contour ~1.1°) of the beams in one frame extracted from the narrow-field CMOS camera measurements used in the study by *Dahlgren et al*. [2013], with geodetic azimuth and elevation contours shown. The narrow-field camera was collocated with PFISR; thus, the beam patterns in Figure 1 are independent of the altitude.

The magnetic-zenith beam, indicated in solid red, is defined as the radar beam parallel to the magnetic field line at the ground, as determined using the International Geomagnetic Reference Field model [*International Association of Geomagnetism and Aeronomy*, *Working Group V-MOD*, 2010]. Due to curvature of the field lines, this beam is not exactly parallel to the field lines at higher altitudes. However, it remains the closest beam to parallel. At altitudes where the NEIALs are observed, the magnetic-zenith beam has an angle of about 0.2° with the magnetic field lines.

A substorm onset occurred in the southeast of the PFISR facility at ~10:00 UT on 1 March 2011, with the poleward expansion of the aurora reaching the PFISR zenith at ~10:05:30 UT. Figure 2 shows snapshots at 557.7 nm wavelength recorded by the Poker Flat all-sky camera as the aurora expanded through the PFISR

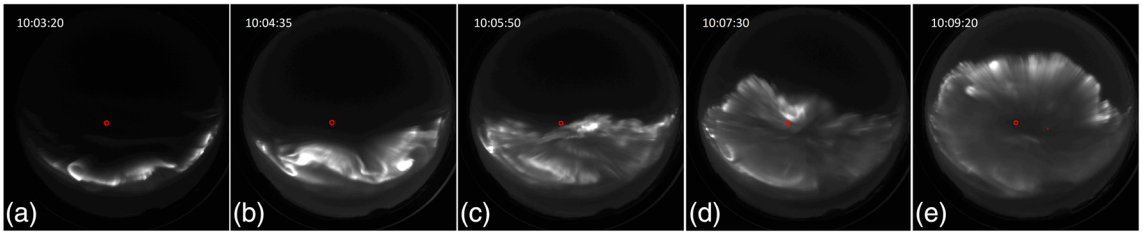

Figure 2. (a–e) Sequential all-sky camera samples showing auroral activity associated with a substorm poleward expansion on 1 March 2011. The nominal position of the PFISR beam cluster (Figure 1) is indicated in red.

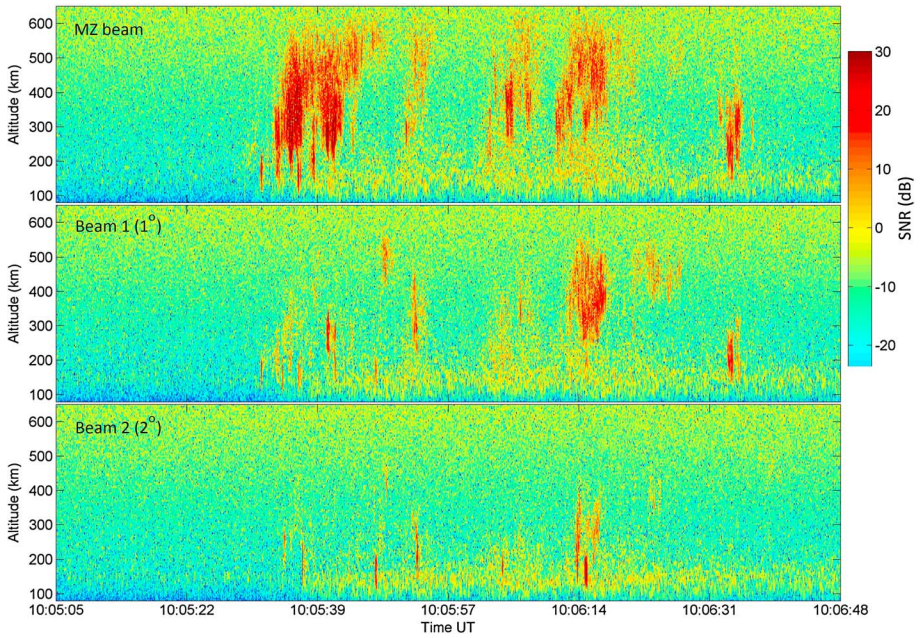

Figure 3. Range-time plot of received power in the ion line channel for three of the radar beams (see Figure 1) during a period when the substorm expansion crossed through the PFISR beams. Mentioned in parentheses are angles with respect to the magnetic-zenith beam.

beam cluster (indicated in red). The oxygen 557.7 nm emission in the aurora occurs at altitudes between 120 and 180 km. It is a proxy for electron precipitation over a broad range of energies and is therefore expected to appear on flux tubes that are magnetically conjugate to NEIALs.

Figure 3 shows received PFISR power in the ion line channel during this period. For the sake of simplifying the aspect angle comparison, radar data in only three beams are shown, corresponding to the beams labeled MZ, 1, and 2 in Figure 1. The streaks with power >10 dB are all NEIALs. Significant variations in the echo power are observed from beam to beam. The echoes at higher altitudes (>250 km) in the zenith beam are less pronounced at 1° offset and almost completely disappear at 2° offset. The angular dependence is less significant for the lower altitude echoes (<250 km). This is readily seen in Figure 4, which shows line plots of the occurrence rate of NEIALs for all five beams during a 90 s period starting at 10:05:20 UT. The occurrence rate at any altitude is calculated by counting the transmitted radar pulses from Figure 3 for which the scattered power from the same altitude is at least a factor of 10 higher than thermal level. The values are then normalized with total number of transmitted radar pulses during this 90 s interval.

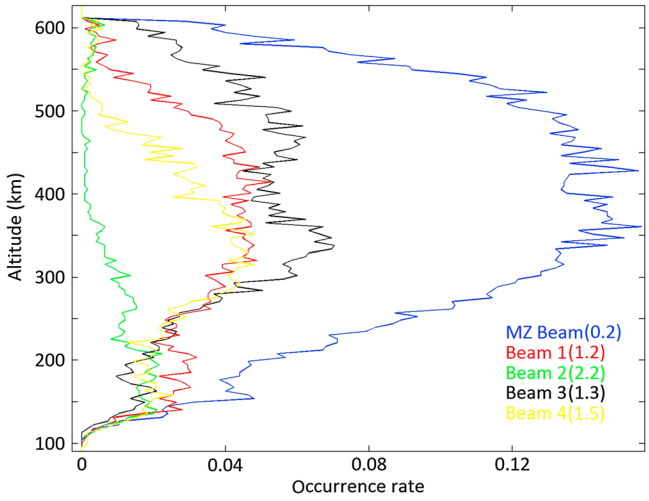

Figure 4. Line plots of relative occurrence of NEIALs during a 90 s period starting at 10:05:20 UT for all beams of the 1 March 2011 experiment. Mentioned in parentheses are angles with respect to magnetic field line at 500 km.

An overview movie showing the full all-sky camera image sequence used to create Figure 2 and the corresponding PFISR backscattered power measurements, embodying the interval of Figure 3, has been included in the supporting information. The movie

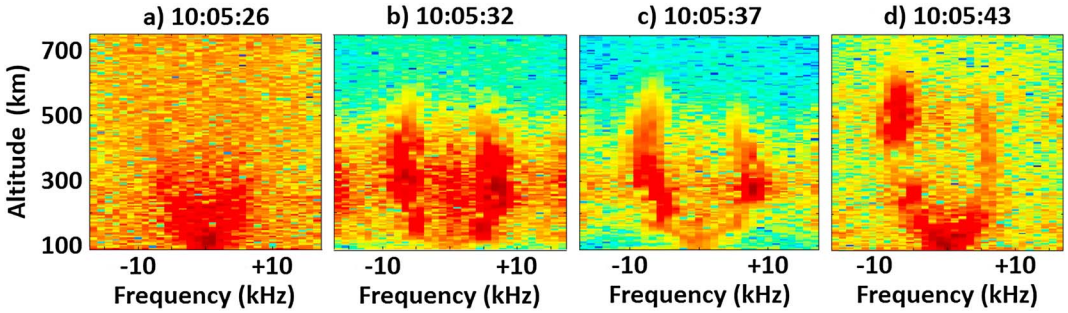

Figure 5. (a–d) Samples of normalized PFISR power spectra corresponding to Figure 3, computed using only 5 s integration and 71 radar pulses. Figure 5a shows the preevent thermal backscatter. Figures 5b–5d exhibit various types of enhancements in the ion acoustic lines. The time stamps correspond to the start time of the integration.

better illustrates the space-time relationship between poleward expanding auroral forms and the occurrence of NEIALs within the PFISR beam cluster.

Figure 5 shows 5 s samples of the zenith ion line power as a function of frequency and altitude. Each image has been individually normalized in order to highlight morphological variations. Figure 5a corresponds to preevent conditions and represents thermal ISR scatter. Figure 5b corresponds to the poleward edge of the substorm expansion, showing enhancements in both ion line shoulders with some evidence for a zero-Doppler central peak. Presence of a zero-Doppler central peak in ion line spectra has been previously observed and explained in terms of the cavitating Langmuir turbulence [*Guio and Forme*, 2006; *Akbari et al*., 2012; *Isham et al*., 2012]. Figures 5c and 5d show the evolution toward higher-altitude echoes, with preferential enhancement of the downshifted shoulder. Figure 5d shoulders exhibit a negative bulk Doppler shift, corresponding to upward ion velocities of ~800 m/s at 500 km altitude.

Although the standard ISR analysis used to derive plasma parameters is not applicable for the coherent echoes, the frequency offset of the ion acoustic shoulders can be used to determine the wave phase velocity and, therefore, the plasma temperatures. Following the procedure presented by *Forme and Fontaine* [1999], for the echoes below 200 km the location of the shoulders at ±6 kHz and ion composition of mixture of NO^+ and O_2^+ and the further assumption that the ion temperature maintains its typical value of ~ 1100 K just before the occurrence of the turbulence [*Forme and Fontaine*, 1999] gives the estimation of $T_e \approx 5000$ K. For the echoes above 200 km, the shoulder offset is 9 kHz. Assuming that O^+ is the dominant ion with a temperature of ~ 2000 K, we again calculate $T_e \approx 5000$ K.

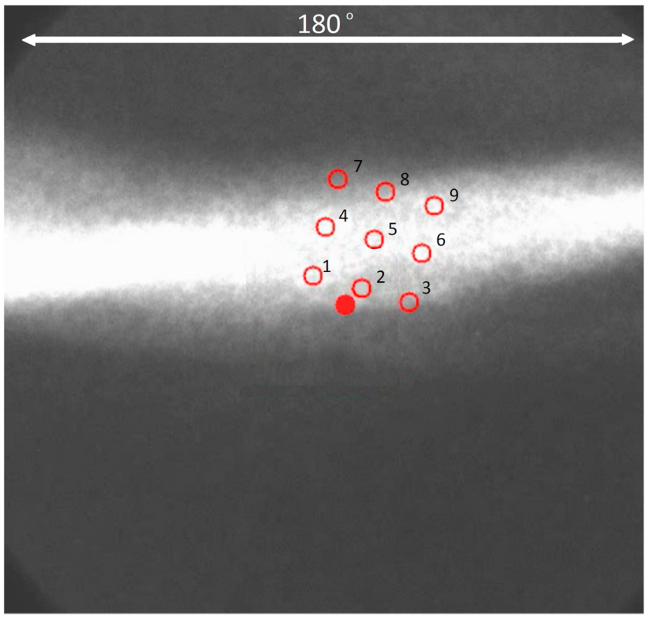

Figure 6. Radar beams configuration on top of one frame of an all-sky camera (23 March 2007 experiment). The magnetic-zenith beam is filled in.

In an attempt to further explore magnetic aspect angle dependence, we studied results obtained from another multibeam PFISR experiment conducted on 23 March 2007. This time, PFISR was configured to sample a 3×3 array of beam positions plus an additional beam trained in the magnetic zenith. Similar to Figure 1, Figure 6 shows the position of the radar beams on a sample auroral image, with the magnetic-zenith beam marked and other beams numbered 1–9. At

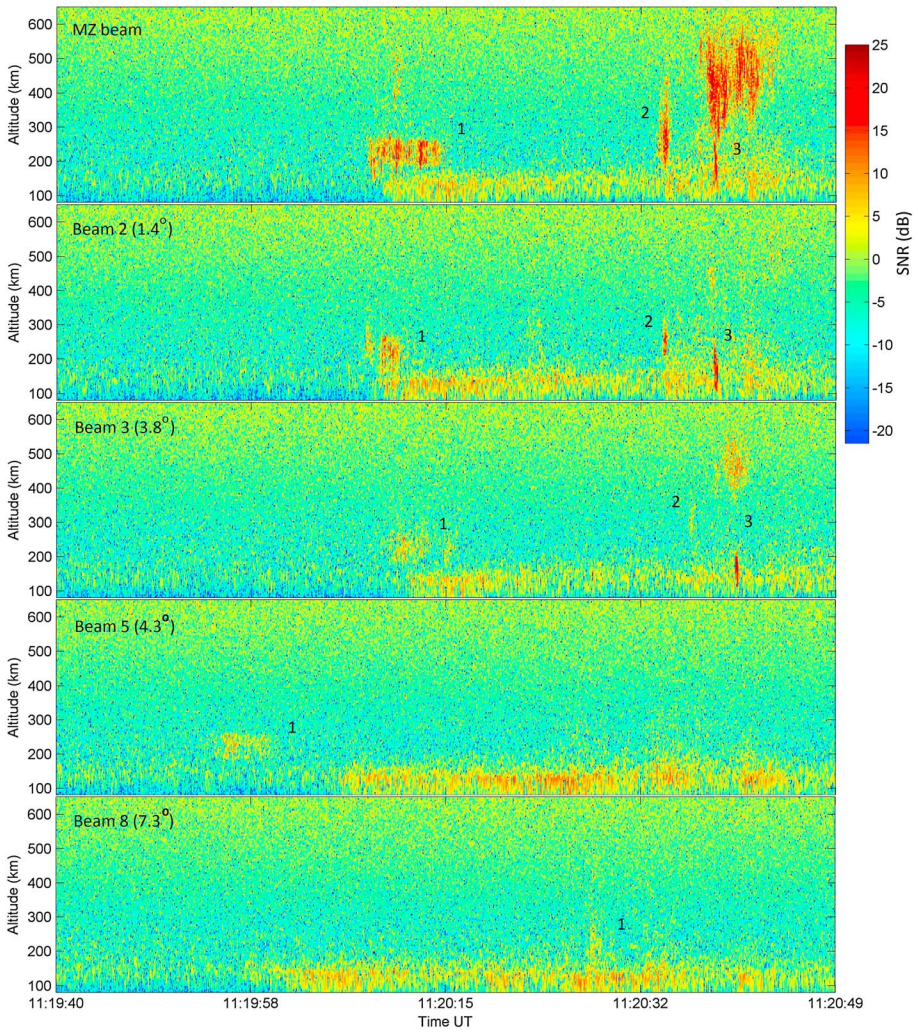

Figure 7. (first to fifth rows) Similar to Figure 3, range-time plot of received power in ion line channel for five of the radar beams in Figure 6. Mentioned in parentheses are angles with respect to the magnetic-zenith beam. In Figure 7 (first row), three bursts of coherent echoes are labeled (echo 3 refers to the whole enhanced received power extended from 100 to 600 km), which are tracked in subsequent rows. Echoes similar to echo 1 appear in all rows while echoes similar to echo 3 only appear in Figure 7 (first to third rows) (see *Akbari et al*. [2012, 2013] and *Semeter et al*., [2008] for further discussion of these data).

~11:20:10 UT, strong echoes were observed in seven beams. Figure 7 shows the total received ion line power as a function of altitude and time in the five radar beams (beams MZ, 2, 3, 5, and 8) where the coherent echoes are strongest. In the magnetic-zenith beam three bursts of echoes are identified and numbered. These echoes were discussed in detail by *Akbari et al*. [2012], and the discussion will not be repeated here. However, for convenience, ion line spectra associated with echo 1 and echo 3 are shown in Figure 8. In short, the filled-in ion line spectrum characteristic of echo 1 (hereafter called type 1) and the simultaneous observation of a double-peaked plasma line spectrum led to the conclusion that this echo was produced by strong Langmuir turbulence [*Akbari et al*., 2012]. The characteristics of echo 3 (hereafter called type 2), however, were similar to characteristics of the echoes in Figures 3 and 5. The high altitude portion of this spectrum can be seen to be Doppler shifted by about 2 kHz toward negative frequencies, indicating upward motion of plasma with velocity of ~660 m/s.

Comparing Figure 7 to Figure 3, we find similar aspect angle dependence: (1) there is a decrease in NEIAL visibility with increased aspect angle and (2) the higher-altitude type 2 echoes show stronger aspect angle sensitivity than the lower altitude type 2 and type 1 echoes.

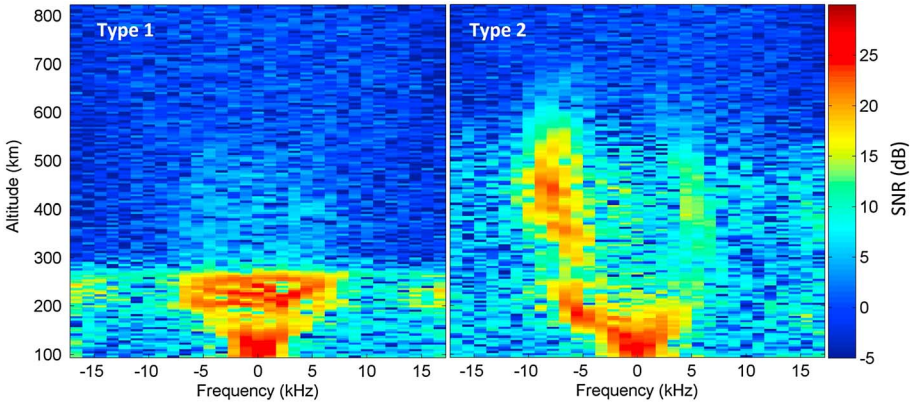

Figure 8. Ion line spectra computed from measurements within the first and third echoes in Figure 7 (first row). The apparent shift of the type 2 spectrum toward negative frequencies corresponds to upward plasma velocity of ~660 m/s.

3. Discussion

Using the European Incoherent Scatter UHF radar *Rietveld et al*. [1991] reported NEIALs at angles 0, 12.5, and 14.6° with respect to magnetic field lines and found the main difference to be a smaller range extent of NEIALs at larger angles. The results were explained in terms of the horizontally localized nature of NEIALs. Our results, obtained using pulse-by-pulse sampling with the electronically steerable PFISR, show a significant difference in NEIAL power for beams that are separated by only 1°.

The claim rests on the combined consideration of radar and all-sky camera observations. In carefully examining Figure 3, for instance, one does not find one-to-one correlation between features observed at different aspect angles. This is not surprising, since the horizontal extent of individual NEIAL scattering regions is small (~100 m) compared to the beam separation (~5 km at 300 km range). However, a clear trend can be seen in the observability of NEIALs as the radar beam moves away from parallel to the magnetic field lines; that is, the NEIALs at higher altitudes quickly disappear as the angle increases.

There are two possible explanations for this trend. One is that the source of the NEIALs was nonuniformly distributed within the spatial region covered by the different beams. But this is not supported by the optical measurements. Figure 2 showed representative auroral activity recorded before, during, and after the interval shown in Figure 3. In Figure 2a, at 10:03:20 UT, electron precipitation, manifested by auroral brightness, was present in the south and spread toward the north. At time 10:05:50 UT, corresponding to Figure 2c, the poleward edge of the brightness reached the region intersected by the PFISR beams, and the NEIAL echoes appeared in radar data. As the leading edge of the substorm expansion continued poleward, past the PFISR beams, the coherent echoes disappeared. There is no reason to believe that the characteristics of the NEIAL source changed as the source traversed the PFISR beam pattern. This conclusion is further supported by Movie S1 in the supporting information, which shows a longer interval of PFISR backscattered power measurements in the magnetic zenith and the corresponding full all-sky image sequence (20 s samples). We therefore conclude that the second explanation is more plausible, namely, the observed trend reveals variations in the observability of NEIALs with magnetic aspect angle.

The aspect angle dependence of NEIALs is determined by their generation mechanism. Strong dependence is not expected for NEIALs produced by the parametric decay of Langmuir waves. In both weak and strong Langmuir turbulence regimes, even if the initial Langmuir wave produced by an electron beams is strictly field aligned, the interaction of the Langmuir waves and ion density perturbations spreads the energy to larger angles, and as a result, incoherent scatter radars would be expected to observe the turbulence at angles as high as 20 and 40° for the weak and strong regimes of turbulence, respectively [*DuBois et al*., 1993]. Note that the angular spread of turbulence also depends strongly on the source intensity, and for very small source energies the angular spread might not be as high as the angles mentioned above. Therefore, the aspect angle dependence seen in Figure 3 strongly suggests that these echoes are not produced by parametric decay of Langmuir waves but, rather, are produced by a plasma streaming instability.

In previous observational studies, the simultaneous enhancement of both ion acoustic shoulders, the rapid successive appearance of upshifted and downshifted shoulder at similar altitudes, and the asymmetry sometimes found in altitude profiles of NEIALs [*Forme et al*., 2001] have been used to argue in favor of the parametric decay mechanism. In our observations, however, the same arguments fail to explain the dominance of the enhanced downshifted shoulder (corresponding to upward wave propagation) at the highest altitudes (>550 km). Moreover, coherent echoes produced by the Langmuir decay mechanism are most expected in a narrow layer around the *F* region peak, where the effect of the density gradient in saturating the wave amplitude is minimum [*Akbari et al*., 2013]. Finally, noting the fact that type 2 NEIALs occur over large altitude extents, one would expect to detect concurrent plasma line enhancements if the NEIALs were indeed produced by parametric decay. Although the ion acoustic wave and the Langmuir waves involved in a parametric decay have different wave numbers and ISRs only observe wave activity in a single wave number, the presence of the echoes from 600 km all the way down to 150 km (i.e., more than a factor of 4 range in plasma density) implies that the Langmuir waves are subject to instability over a wide range of wave numbers. This wide range of plasma densities should guarantee the simultaneous observation of NEIALs at higher altitudes and Langmuir waves near the *F* region peak.

On the other hand, the simultaneous enhancement of both ion acoustic shoulders along with the observed upward plasma motion of ~660 m/s (Figure 8, right) argues in favor of the ion-ion streaming instability mechanism [*Wahlund et al*., 1992] for the type 2 echoes above 200 km (note that unless subjected to temporal/spatial averaging, electron-ion streaming instability cannot give rise to simultaneous enhancement of both ion acoustic shoulders). The observed upward plasma motion is also consistent with the high ion temperatures derived for lower altitudes. Ion temperature enhancements can be produced by strong horizontal electric fields that are often observed on the edge of auroral arcs and subsequent ion-neutral frictional heating due to $\mathbf{E} \times \mathbf{B}$ drift [*Lynch et al*., 2007; *Zettergren et al*., 2008]. Alternatively, the ion heating and the upward motion can be produced by the electrostatic ion cyclotron instability on the boundary of auroral precipitations [*Ungstrup et al*., 1979; *Bering*, 1984; *Lysak et al*., 1980; *Palmadesso et al*., 1974].

Although plausible for higher-altitude (>200 km) type 2 NEIALs, the ion-ion streaming instability mechanism does not suit the lower altitude (<200 km) type 2 NEIALs (shown in Figure 3). First, no sign of vertical plasma motion exists; second, ion acoustic shoulders are not enhanced simultaneously; and third, at these altitudes ion dynamics are dominated by ion-neutral collision that prevents any mechanism from producing relative drift between different ion species. Observations of NEIALs at such low altitudes are rare. In fact, we are only aware of those reported by *Rietveld et al*. [1991]. In their observations, given the fact that only the upshifted shoulder was enhanced at lower altitudes, they argued that the echoes were produced by thermal electrons streaming from the *F* region toward the *E* region. According to this theory, soft electron precipitation is collisionally stopped at *F* region heights where cross-field mobility is poor. Accumulation of electrons results in a field-aligned electric field which, in turn, repels thermal electrons upward and downward from the stopping height. This mechanism may be applicable to the Rietveld et al. observations but cannot explain the low-altitude downshifted shoulder enhancements observed in our data. The ion cyclotron mechanism proposed by *Bahcivan and Cosgrove* [2008] or upward streaming thermal electrons originating from even lower altitudes might be candidate mechanisms.

The weaker aspect angle dependence of type 2 echoes at lower altitudes versus at higher altitudes should be further studied. Whether this is due to a different generation mechanism or due to parameters of the ambient plasma is yet to be determined. However, we would like to mention the possibility that this behavior might be simply due to different plasma parameters at lower and higher altitudes rather than the source of instabilities. At lower altitudes, the ions become increasingly demagnetized and their motions are not as tightly constrained by the magnetic field compared with higher altitudes. As a result, ion acoustic turbulence might be less sensitive to magnetic aspect angle at lower altitudes.

4. Conclusion

Experimental data presented in this report reveals that the visibility of substorm-related NEIALs by incoherent scatter radars is highly sensitive to magnetic aspect angle. The aspect angle sensitivity was found to depend on both altitude and spectral morphology, providing a means of classifying the results according to allowable generation mechanisms: type 1 NEIALs (flat ion line spectrum) are consistent with the parametric decay of

Langmuir waves into ion acoustic waves, and these echoes show weak aspect angle dependence. The higher-altitude (>200 km) type 2 NEIALs (one or both ion acoustic shoulders enhanced) are consistent with the ion-ion streaming instability and are extremely sensitive to the aspect angle. These echoes almost completely disappear when the aspect angle is increased to only 2°. And finally, the lower altitude (<200 km) type 2 NEIALs show less aspect angle sensitivity when compared to the higher-altitude type 2 NEIALs; these echoes are not consistent with the ion-ion streaming instability. We also conclude that during dynamic geophysical conditions, such as the substorm intervals studied in this report, more than one of the generation mechanisms proposed to explain NEIALs may be simultaneously at work.

Acknowledgments

The authors are grateful to Michael Nicolls and the SRI Center for Geospace Science for PFISR experimental support and Don Hampton (Geophysical Institute, University of Alaska) for access to the all-sky camera data. This research was supported by the National Science Foundation under grants AGS-1244675 and AGS-1339500 and by the Air Force Office of Scientific Research under contract FA9550-12-1-018.

Michael Liemohn thanks the reviewers for their assistance in evaluating the paper.

References

Akbari, H., J. L. Semeter, H. Dahlgren, M. Diaz, M. Zettergren, A. Strømme, M. J. Nicolls, and C. Heinselman (2012), Anomalous ISR echoes preceding auroral breakup: Evidence for strong Langmuir turbulence, *Geophys. Res. Lett.*, *39*, L03102, doi:10.1029/2011GL050288.

Akbari, H., J. L. Semeter, M. J. Nicolls, M. Broughton, and J. W. LaBelle (2013), Localization of auroral Langmuir turbulence in thin layers, *J. Geophys. Res. Space Physics*, *118*, 3576–3583, doi:10.1002/jgra.50314.

Bahcivan, H., and R. Cosgrove (2008), Enhanced ion acoustic lines due to strong ion cyclotron wave fields, *Ann. Geophys.*, *26*, 2081–2095.

Bering, E. A. (1984), The plasma wave environment of an auroral arc: Electrostatic ion cyclotron waves in the diffuse aurora, *J. Geophys. Res.*, *89*(A3), 1635–1649, doi:10.1029/JA089iA03p01635.

Blixt, E. M., T. Grydeland, N. Ivchenko, T. Hagfors, C. La Hoz, B. S. Lanchester, U. P. Løvhaug, and T. S. Trondsen (2005), Dynamic rayed aurora and enhanced ionacoustic radar echoes, *Ann. Geophys.*, *23*, 3–11.

Cabrit, B., H. Opgenoorth, and W. Kofman (1996), Comparison between EISCAT UHF and VHF backscattering cross section, *J. Geophys. Res.*, *101*(A2), 2369–2376, doi:10.1029/95JA02175.

Collis, P. N., I. Häggström, K. Kaila, and M. T. Rietveld (1991), EISCAT radar observations of enhanced incoherent scatter spectra: Their relation to red aurora and field-aligned currents, *Geophys. Res. Lett.*, *18*(6), 1031–1034, doi:10.1029/91GL00848.

Dahlgren, H., J. L. Semeter, R. A. Marshall, and M. Zettergren (2013), The optical manifestation of dispersive field-aligned bursts in auroral breakup arcs, *J. Geophys. Res. Space Physics*, *118*, 4572–4582, doi:10.1002/jgra.50415.

Dubois, D. F., A. Hanssen, H. A. Rose, and D. Russell (1993), Space and time distribution of HF excited Langmuir turbulence in the ionosphere: Comparison of theory and experiment, *J. Geophys. Res.*, *98*(A10), 17,543–17,567, doi:10.1029/93JA01469.

Forme, F., and D. Fontaine (1999), Enhanced ion acoustic fluctuations and ion outflows, *Ann. Geophys.*, *17*, 182, doi:10.1007/s00585-999-0182-6.

Forme, F., Y. Ogawa, and S. C. Buchert (2001), Naturally enhanced ion acoustic fluctuations seen at different wavelengths, *J. Geophys. Res.*, *106*(A10), 21,503–21,515, doi:10.1029/2000JA900164.

Forme, F. R. E. (1993), A new interpretation on the origin of enhanced ion-acoustic fluctuations in the upper atmosphere, *Geophys. Res. Lett.*, *20*(21), 2347–2350, doi:10.1029/93GL02490.

Forme, F. R. E. (1999), Parametric decay of beam-driven Langmuir waves and enhanced ion-acoustic fluctuations in the ionosphere: A weak turbulence approach, *Ann. Geophys.*, *17*, 1172–1181.

Foster, J. C., C. del Pozo, K. Groves, and J.-P. Saint Maurice (1988), Radar observations of the onset of current driven instabilities in the topside ionosphere, *Geophys. Res. Lett.*, *15*(2), 160–163, doi:10.1029/GL015i002p00160.

Grydeland, T., C. La Hoz, T. Hagfors, E. M. Blixt, S. Saito, A. Strømme, and A. Brekke, (2003), Interferometric observations of filamentary structures associated with plasma instability in the auroral ionosphere. *Geophy. Res. Lett. 30*(6), 1338, doi:10.1029/2002GL016362.

Grydeland, T., E. Blixt, U. Løvhaug, T. Hagfors, C. La Hoz, and T. Trondsen (2004), Interferometric radar observations of filamented structures due to plasma instabilities and their relation to dynamic auroral rays, *Ann. Geophys.*, *22*, 1115–1132.

Guio, P. and F. Forme (2006), Zakharov simulations of Langmuir turbulence: Effects on the ion-acoustic waves in incoherent scattering. *Phys. Plasmas*, *13*, 122902, doi:10.1063/1.2402145.

International Association of Geomagnetism and Aeronomy, Working Group V-MOD (2010), International Geomagnetic Reference Field: The eleventh generation, *Geophys. J. Int.*, *183*, 1216–1230, doi:10.1111/j.1365-246X.2010.04804.x.

Isham, B., M. T. Rietveld, P. Guio, F. R. E. Forme, T. Grydeland, and E. Mjolhus (2012), Cavitating Langmuir turbulence in the terrestrial aurora, *Phys. Rev. Lett.*, *108*, 105003, doi:10.1103/PhysRevLett.108.105003.

Lynch, K. A., J. Semeter, M. Zettergren, P. Kintner, R. Arnoldy, E. A. MacDonald, E. Klatt, J. LaBelle, and M. Samara (2007), Auroral ion outflow: Low altitude energization, *Ann. Geophys.*, *25*, 1959–1965.

Lysak, R., M. Hudson, and M. Temerin (1980), Ion heating by strong electrostatic ion cyclotron turbulence, *J. Geophys. Res.*, *85*(A2), 678–686, doi:10.1029/JA085iA02p00678.

Michell, R. G., and M. Samara (2010), High-resolution observations of naturally enhanced ion acoustic lines and accompanying auroral fine structures, *J. Geophys. Res.*, *115*, A03310, doi:10.1029/2009JA014661.

Michell, R. G., K. A. Lynch, C. J. Heinselman, and H. C. Stenbaek-Nielsen (2008), PFISR nightside observations of naturally enhanced ion acoustic lines, and their relation to boundary auroral features, *Ann. Geophys.*, *26*, 3623–3639.

Michell, R. G., K. A. Lynch, C. J. Heinselman, and H. C. Stenbaek-Nielsen (2009), High time resolution PFISR and optical observations of naturally enhanced ion acoustic lines, *Ann. Geophys.*, *27*, 1457–1467.

Palmadesso, P. J., T. P. Coffey, S. L. Ossakow, and K. Papadopoulos (1974), Topside ionosphere ion heating due to electrostatic ion cyclotron turbulence, *Geophys. Res. Lett.*, *1*(3), 105–108, doi:10.1029/GL001i003p00105.

Rietveld, M. T., P. N. Collis, and J.-P. St.-Maurice (1991), Naturally enhanced ion acoustic waves in the auroral ionosphere observed with the EISCAT 933-MHz radar, *J. Geophys. Res.*, *96*(A11), 19,291–19,305, doi:10.1029/91JA01188.

Rietveld, M. T., P. N. Collis, A. P. van Eyken, and U. P. Løvhaug (1996), Coherent echoes during EISCAT UHF common programs, *J. Atmos. Sol. Terr. Phys.*, *58*, 161–174.

Sedgemore-Schulthess, K. J. F., M. Lockwood, T. S. Trondsen, B. S. Lanchester, M. H. Rees, D. A. Lorentzen, and J. Moen (1999), Coherent EISCAT Svalbard Radar spectra from the dayside cusp/cleft and their implications for transient field-aligned currents, *J. Geophys. Res.*, *104*(A11), 24,613–24,624, doi:10.1029/1999JA900276.

Semeter, J., M. Zettergren, M. Diaz, and S. Mende (2008), Wave dispersion and the discrete aurora: New constraints derived from high-speed imagery, *J. Geophys. Res.*, *113*, A12208, doi:10.1029/2008JA013122.

Strømme, A., V. Belyey, T. Grydeland, C. La Hoz, U. P. Løvhaug, and B. Isham (2005), Evidence of naturally occurring wave-wave interactions in the polar ionosphere and its relation to naturally enhanced ion acoustic lines, *Geophys. Res. Lett.*, *32*, L05103, doi:10.1029/2004GL020239.

Ungstrup, E., D. M. Klumpar, and W. J. Heikkila (1979), Heating of ions to superthermal energies in the topside ionosphere by electrostatic ion cyclotron waves, *J. Geophys. Res.*, *84*(A8), 4289–4296, doi:10.1029/JA084iA08p04289.

Wahlund, J.-E., F. R. E. Forme, H. J. Opgenoorth, M. A. L. Persson, E. V. Mishin, and A. S. Volotkin (1992), Scattering of electromagnetic waves from a plasma: Enhanced ion-acoustic fluctuations due to ion-ion two-stream instabilities, *Geophys. Res. Lett.*, *19*(19), 1919–1922, doi:10.1029/92GL02101.

Zettergren, M., J. Semeter, P.-L. Blelly, G. Sivjee, I. Azeem, S. Mende, H. Gleisner, M. Diaz, and O. Witasse (2008), Optical estimation of auroral ion upflow: 2. A case study, *J. Geophys. Res.*, *113*, A07308, doi:10.1029/2008JA013135.